Comparisons between different techniques for measuring mass segregation

Richard J. Parker[1]* and Simon P. Goodwin[2]

[1] *Astrophysics Research Institute, Liverpool John Moores University, 146 Brownlow Hill, Liverpool, L3 5RF, UK*
[2] *Department of Physics and Astronomy, University of Sheffield, Sheffield, S3 7RH, UK*

11 March 2015

ABSTRACT

We examine the performance of four different methods which are used to measure mass segregation in star-forming regions: the radial variation of the mass function $\mathcal{M}_{\rm MF}$; the minimum spanning tree-based $\Lambda_{\rm MSR}$ method; the local surface density $\Sigma_{\rm LDR}$ method; and the $\Omega_{\rm GSR}$ technique, which isolates groups of stars and determines whether the most massive star in each group is more centrally concentrated than the average star. All four methods have been proposed in the literature as techniques for quantifying mass segregation, yet they routinely produce contradictory results as they do not all measure the same thing. We apply each method to synthetic star-forming regions to determine when and why they have shortcomings. When a star-forming region is smooth and centrally concentrated, all four methods correctly identify mass segregation when it is present. However, if the region is spatially substructured, the $\Omega_{\rm GSR}$ method fails because it arbitrarily defines groups in the hierarchical distribution, and usually discards positional information for many of the most massive stars in the region. We also show that the $\Lambda_{\rm MSR}$ and $\Sigma_{\rm LDR}$ methods can sometimes produce apparently contradictory results, because they use different definitions of mass segregation. We conclude that only $\Lambda_{\rm MSR}$ measures mass segregation in the classical sense (without the need for defining the centre of the region), although $\Sigma_{\rm LDR}$ does place limits on the amount of previous dynamical evolution in a star-forming region.

Key words: stars: formation – star clusters: general

1 INTRODUCTION

Most young ($<10\,{\rm Myr}$) stars are observed in the company of others, either in clusters (Lada & Lada 2003), groups (Porras et al. 2003), associations (Blaauw 1964) or in regions which are over-dense with respect to the Galactic field (Bressert et al. 2010). Attempts have been made at distinguishing isolated versus clustered star-formation, or clusters versus associations (e.g. Cartwright & Whitworth 2004; Gieles & Portegies Zwart 2011). However, it appears that (at least on local scales) there is no fundamental scale unit for star formation (e.g. Bressert et al. 2010), and that clusters may just be the dense tail of the distribution of Galactic star formation (Kruijssen 2012).

Given that star formation on pc-scales often seems to produce complex, hierarchical distributions, it is crucial to be able to examine the spatial distributions of stars in a quantitative, statistical way. This allows us to extract information on star formation and compare and contrast different regions (and simulations). One such indicator is the relative positions of the most massive stars with respect to the average stars in a region – often referred to as 'mass segregation' when the most massive stars are more centrally concentrated than average.

In recent years several alternative methods for measuring mass segregation have been proposed in the literature. In this paper we critically assess several of the new methods, including the $\Lambda_{\rm MSR}$ method (Allison et al. 2009), the $\Sigma - m$ or $\Sigma_{\rm LDR}$ method (Maschberger & Clarke 2011) and the technique of dividing a star-forming region into groups to determine the relative distance of the most massive star to the centre of each group (Kirk & Myers 2011; Kirk et al. 2014), which we call $\Omega_{\rm GSR}$. A similar study to compare mass segregation methods was previously carried out by Olczak et al. (2011); however, the $\Sigma_{\rm LDR}$ and $\Omega_{\rm GSR}$ methods were not yet prominent in the literature and therefore not included in that study. A full appraisal of these methods – and $\Lambda_{\rm MSR}$ – using synthetic data is therefore required in order to make sense of the growing literature in this area.

The paper is organised as follows. In Section 2 we provide a brief summary of the different methods used to define mass segregation, and discuss the methods we will use in this

* E-mail: R.J.Parker@ljmu.ac.uk

paper in detail. In Section 3 we test these methods on synthetic data, before discussing our results in Section 4 and concluding in Section 5.

2   WHAT IS MASS SEGREGATION?

'Mass segregation' is a phrase often used in relation to star clusters and regions, but often it is not defined.

The classical definition of mass segregation is based on the behaviour of dynamically old bound systems (i.e. relaxed and virialised star clusters). The process of two-body relaxation redistributes energy between stars and they approach energy equipartition whereby all stars have the same mean kinetic energy – this means that more massive stars will have a velocity dispersion that is lower. Because the velocity dispersion of the more massive stars is lower, they will tend to be concentrated towards the centre of the cluster (Spitzer 1969).

The timescale, $t_{\mathrm{MS}}(M)$, on which stars of mass M will dynamically mass segregate depends on the mean mass of stars $\langle m \rangle$ and the two-body relaxation time, t_{relax} (Spitzer 1969)

$$t_{\mathrm{MS}}(M) \sim \frac{M}{\langle m \rangle} t_{\mathrm{relax}}. \tag{1}$$

Therefore in old star clusters (especially globular clusters) we expect to see mass segregation down to low masses and that mass segregation is explicable entirely by dynamics.

In these old clusters, the two-body dynamics that may have caused any mass segregation will also remove any primordial substructure in the spatial distribution and we would expect (and observe) the cluster to have a smooth, centrally concentrated spatial distribution, such as a Plummer (1911) or King (1966) profile.

In this case, the clusters have a well-defined radial profile where one can quantify mass segregation by taking different mass bins and comparing the density profiles (e.g. Hillenbrand 1997; Pinfield et al. 1998), or examining variations in the slope of the mass function (or luminosity function) with distance from the cluster centre (Carpenter et al. 1997; de Grijs et al. 2002; Gouliermis et al. 2004). A related method is to quantify the variation of the 'Spitzer radius' – the rms distance of stars in a cluster around the centre of mass – with luminosity (Gouliermis et al. 2009).

The motivation in attempting to observe mass segregation in young clusters or regions is that it might not have a dynamical origin. If we observe mass segregation in a region that is so young that two-body encounters cannot have mass segregated the stars[1], then the mass segregation must be set by some aspect of the star formation process, and is often labelled 'primordial mass segregation'.

Primordial mass segregation has been found in some simulations of star formation (e.g. Maschberger & Clarke 2011; Myers et al. 2014) but not in others (Girichidis et al. 2012; Parker et al. 2015), and we also note that any observed signature may be a combination of primordial and dynamical mass segregation (Moeckel & Bonnell 2009), and

to complicate matters further mass segregation can be introduced very rapidly dynamically through violent relaxation rather than two-body relaxation (see Allison et al. 2010).

Observationally, mass segregation has been searched for in clusters and star forming regions for many years (e.g. Sagar et al. 1988; de Marchi & Paresce 1996; Hillenbrand & Hartmann 1998; Raboud & Mermilliod 1998; de Grijs et al. 2002; Gouliermis et al. 2004; Sabbi et al. 2008; Gouliermis et al. 2009, and many more), but in the past few years a number of new statistical methods have been developed for finding mass segregation, and the purpose of this paper is to examine what *exactly* they are searching for, and what problems they might have.

Here we briefly describe the most commonly used methods and their assumptions. In the next section we describe exactly how we implement each method in detail.

It should be noted that all methods suffer from a potentially very serious problem. All methods examine the relative distributions of high- and low-mass stars. Therefore the distribution of low-mass stars must be known, however these are very faint compared to the high-mass stars in young regions/clusters. And so the location in which the observer is biased against observing low-mass stars is near luminous high-mass stars which is exactly where one needs to know if low-mass stars are present or not. In this paper we use fake data in which we have the advantage of knowing exactly where every star is and what its mass is, but real observations do not have this advantage (see Stolte et al. 2005; Ascenso et al. 2009, for a detailed discussion of observational selection effects and biases).

2.1   Radial mass functions, $\mathcal{M}_{\mathrm{MF}}$

Until recently, the most commonly used way of determining mass segregation was to compare the radial distribution of the mass function, or the radial distribution of stars of different masses (e.g. Sagar et al. 1988; Gouliermis et al. 2004; Stolte et al. 2006; Sabbi et al. 2008; Chavarría et al. 2010). In this definition, if a cluster is mass segregated the most massive stars are preferentially towards the centre, and low-mass stars preferentially in the outskirts. Therefore the slope of the mass function should be flatter in the centre than the outskirts, and/or the low-mass stars should have a much broader radial distribution.

This method suffers three significant drawbacks. One is that it requires a 'centre' to be defined. In relaxed, virialised star clusters there is a centre from which this can be measured, but in substructured and messy young star forming regions it is unclear if defining a 'centre' means anything at all, and even if it did, it is unclear how one would practically do this. One can define a geometric centre based on the positions of stars, but in some morphologies (as we shall see) this 'centre' is not near to, nor is the central location, of the stars.

Second, the definition of radial bins is non-trivial and often arbitrary, which adds a further level of complexity to the interpretation of any signal.

It also suffers from poor statistics, in that it is unclear how to compare different clusters or provide any *quantitative* information on the mass segregation.

In practice, we compare the cumulative distribution of the radii of the ten most massive stars with the cumulative

---

[1] This is complicated by the fact that it is not the current relaxation time of the region that is important, rather it is how dynamically old the region is (see Allison et al. 2010).

distribution of the radii of all the stars in the distribution. We set the 'centre' of the region to be the (known to us) centre of mass of the region. We gauge the significance of any difference using a Kolmogorov-Smirnov (KS) test, and rather generously use a p-value of < 0.1 as our significance threshold.

2.2 The $\Lambda_{\rm MSR}$-parameter

In order to try and avoid the problems of defining a centre and to produce a quantitative statistic to aid comparisons Allison et al. (2009) introduced the $\Lambda_{\rm MSR}$-parameter.

The $\Lambda_{\rm MSR}$-parameter examines the relative (2D) spatial distributions of the N most massive stars relative to each-other with the spatial distributions of N random stars. This is done by finding the edge length of the minimum spanning tree (MST) that connects the N most massive stars with many MSTs of N random stars.

This has the great advantage that it does not require a centre or any special position to be defined. It also produces a number with associated error that states how much longer or shorter the massive star MST is compared to random MSTs, and how likely it is that this length could be drawn at random from the random MSTs (i.e. how likely is this to occur by random chance).

The $\Lambda_{\rm MSR}$-parameter measures a very similar 'mass segregation' to the classical definition: it examines if the massive stars are closer to each-other than one would expect by random chance. If the massive stars are closer to one another, then the star-forming region is said to be mass segregated.

It practice, we take the ratio of the average (mean) random MST length to the subset MST length, a quantitative measure of the degree of mass segregation (normal or inverse) can be obtained. We first determine the subset MST length, $l_{\rm subset}$. We then determine the average length of sets of $N_{\rm MST}$ random stars each time, $\langle l_{\rm average} \rangle$. There is a dispersion associated with the average length of random MSTs, which is roughly Gaussian and can be quantified as the standard deviation of the lengths $\langle l_{\rm average} \rangle \pm \sigma_{\rm average}$. However, we conservatively estimate the lower (upper) uncertainty as the MST length which lies $1/6$ ($5/6$) of the way through an ordered list of all the random lengths (corresponding to a 66 per cent deviation from the median value, $\langle l_{\rm average} \rangle$). This determination prevents a single outlying object from heavily influencing the uncertainty. We can now define the 'mass segregation ratio' ($\Lambda_{\rm MSR}$) as the ratio between the average random MST pathlength and that of a chosen subset, or mass range of objects:

$$\Lambda_{\rm MSR} = \frac{\langle l_{\rm average} \rangle}{l_{\rm subset}} {}^{+\sigma_{5/6}/l_{\rm subset}}_{-\sigma_{1/6}/l_{\rm subset}}. \qquad (2)$$

A $\Lambda_{\rm MSR}$ of ~ 1 shows that the stars in the chosen subset are distributed in the same way as all the other stars, whereas $\Lambda_{\rm MSR} > 1$ indicates mass segregation and $\Lambda_{\rm MSR} < 1$ indicates inverse mass segregation, i.e. the chosen subset is more widely distributed than the other stars.

Note that a slightly different formulation of $\Lambda_{\rm MSR}$, which uses the geometric mean to define the uncertainties, is available (Olczak et al. 2011), but for the purposes of this paper the original method by Allison et al. (2009) is sufficient.

2.3 The local density ratio, $\Sigma_{\rm LDR}$

Maschberger & Clarke (2011) introduced another measure of mass segregation – the local density ratio. For this the local surface density of every star Σ is found, and the average local surface density of the N most massive stars is compared to the average local surface density of all stars to obtain the 'local surface density ratio', $\Sigma_{\rm LDR}$ (Küpper et al. 2011; Parker et al. 2014). This is able to determine if the most massive stars are in regions of significantly higher (or lower) local surface density than would be expected by random chance. If the most massive stars are in areas of higher local density than the region average, the region is said to be mass segregated.

As with $\Lambda_{\rm MSR}$, $\Sigma_{\rm LDR}$ makes no assumptions about there being a centre. However it is possible that the same numerical value of $\Sigma_{\rm LDR}$ can be statistically significant sometimes, but not other times, which we quantify by means of a KS test.

It is very important to note that $\Lambda_{\rm MSR}$ and $\Sigma_{\rm LDR}$ measure different versions of 'mass segregation'. $\Lambda_{\rm MSR}$ determines if the massive stars are closer to each other than one would expect by random chance, $\Sigma_{\rm LDR}$ determines if the massive stars are in regions of higher surface density than one would expect by random chance.

It would be quite possible for $\Sigma_{\rm LDR}$ to find 'mass segregation', but for $\Lambda_{\rm MSR}$ not to. This would occur for example if the massive stars were widely distributed, but each had a local overdensity of low-mass stars (see Parker et al. 2014, for examples).

In practice, we calculate the local stellar surface density following the prescription of Casertano & Hut (1985), modified to account for the analysis in projection. For an individual star the local stellar surface density is given by

$$\Sigma = \frac{n-1}{\pi r_n^2}, \qquad (3)$$

where r_n is the distance to the $n^{\rm th}$ nearest neighbouring star[2].

Küpper et al. (2011) and Parker et al. (2014) took the ratio of the median surface density of a chosen subset (in this paper we will use the 10 most massive stars) to the median for all stars in a region to define the local surface density ratio, $\Sigma_{\rm LDR}$:

$$\Sigma_{\rm LDR} = \frac{\tilde{\Sigma}_{\rm subset}}{\tilde{\Sigma}_{\rm all}}. \qquad (4)$$

The $\Sigma_{\rm LDR}$ ratio is then quoted with the p-value from the KS test to gauge the significance of any deviation from the median for all stars, again with a p-value < 0.1 used as the boundary between the difference being significant or not.

2.4 Group segregation ratio, $\Omega_{\rm GSR}$

A further, alternative method for quantifying mass segregation was recently suggested by Kirk & Myers (2011) and Kirk et al. (2014). In this method stellar groups are identified and 'isolated' from the total distribution. Each of these

---

[2] Note that this n does not need to have the same value as the N used to define the subset of choice, although we adopt $n = 10$, $N = 10$ throughout this work.

groups is then examined to see if the most massive star it contains is closer to the centre of the group than the median distance of all stars in the group. If the most massive star is closer to the centre than the average star in the majority of the groups, the star-forming region is said to be mass segregated.

The 'mass segregation' searched for in this method is different again from both Λ_{MSR} and Σ_{LDR}. Ω_{GSR} divides the region into groups and then examines each group for evidence of internal mass segregation. In this process many stars in the region (possibly including some of the most massive) can be excluded if they do not belong in a group.

First, an MST is constructed for the entire region and a cumulative distribution of all MST branch lengths is then made. Two power-law slopes are then fitted to the shortest lengths, and the longest lengths, and the intersection of these slopes defines the boundary of subclustering, d_{break} (Gutermuth et al. 2009).

The links in the full MST which exceed d_{break} are removed, resulting in the star-forming region being divided into groups. If the position of the most massive star in the group r_{mm} is closer to the central position than the median value for all stars, r_{med}, the group, or subcluster has an offset ratio (r_{mm}/r_{med}) less than unity and is said to be mass segregated.

In this paper, we define a 'group segregation ratio', Ω_{GSR}, as

$$\Omega_{GSR} = \frac{N_{seg}}{N_{grp}}, \qquad (5)$$

where N_{grp} are the number of groups, and N_{seg} is the number of these groups that have an offset ratio less than unity. If a star-forming region has $\Omega_{GSR} = 1$, then all individual groups defined by d_{break} are mass segregated.

It should be noted that, just by random chance we would expect $\Omega_{GSR} \sim 0.5$, as half of the time the most massive star would be in the inner 50 per cent of stars. The significance of $\Omega_{GSR} \sim 0.5$ is affected by Poisson noise; for example an $\Omega_{GSR} = 0.8$ is not significant if it is 8 out of 10 subgroups.

3   FINDING MASS SEGREGATION IN SIMULATED REGIONS

All of these four methods for finding 'mass segregation' will find classical mass segregation in a relaxed, spatially smooth, spherical, bound cluster. If the most massive stars are close together in the centre of a spherical cluster then: (A) $\mathcal{M}_{MF}$ will show a different mass function in the inner regions. (B) Λ_{MSR} will show that the massive stars are concentrated together. (C) Σ_{LDR} will find that the most massive stars are in the regions of highest surface density. (D) Ω_{GSR} will find that the most massive star is towards the centre of a single group (in this situation, the cluster itself is the group).

In such a situation we would advise the reader to use Λ_{MSR} to look for mass segregation as it gives a single quantitative value for the degree of mass segregation with an associated error, and can easily determine the stellar mass down to which mass mass segregation is present (e.g. Allison et al. 2009; Sana et al. 2010; Beccari et al. 2012; Delgado et al.

2013; Er et al. 2013; Pang et al. 2013; Rivilla et al. 2014; Wright et al. 2014).

What we will examine in this paper is the analysis of complex, substructured regions and the search for 'mass segregation' within them, according to the definition presented in each method.

In this Section we run our four methods for quantifying mass segregation on a synthetic dataset containing $N = 300$ stars to match the small-N statistics of many young regions. We distribute the stars in a fractal distribution according to the prescription in Goodwin & Whitworth (2004), Allison et al. (2010) and Parker et al. (2014). We refer the reader to those papers for a detailed description of how the fractal is set up, but we briefly summarise the method here. The fractal is built by creating a cube containing 'parents', which spawn a number of 'children' depending on the desired fractal dimension, D. The amount of substructure is then set by the number of children that are allowed to mature (the lower the fractal dimension, the fewer children mature and the cube has more substructure).

We choose a fractal distribution because the Λ_{MSR}, Σ_{LDR} and Ω_{GSR} methods were developed specifically to be used on substructured, or hierarchical spatial distributions of stars in star-forming regions and clusters. All three negate the requirement of designating a 'centre' (although the Ω_{GSR} method requires the definition of group centres – as detailed in Section 2.4). Star-formation may result in a truly fractal distribution (Elmegreen & Elmegreen 2001; Cartwright & Whitworth 2004), but star forming regions are unlikely to retain their primordial spatial distribution due to dynamical evolution (Parker et al. 2014). As a default, we choose $D = 2.0$ and assign the fractal a radius of 5 pc.

We note that observed star-forming regions display a range of fractal dimensions (Cartwright & Whitworth 2004; Schmeja et al. 2008, 2009; Sánchez & Alfaro 2009; Gouliermis et al. 2014). It is possible that all regions may form with the same (low) fractal dimension, and observed differences are due to differing amounts of dynamical evolution (Goodwin & Whitworth 2004; Parker et al. 2014; Parker 2014), although simulations of star-formation also produce a range of values before significant dynamical evolution takes place (Girichidis et al. 2012; Dale et al. 2012, 2013). For the purposes of the numerical tests presented here, regions with $D = 2.0$ adequately highlight the differences between the various definitions of mass segregation.

We draw masses from the Maschberger (2013) formulation of the initial mass function (IMF):

$$p(m) \propto \left(\frac{m}{\mu}\right)^{-\alpha} \left(1 + \left(\frac{m}{\mu}\right)^{1-\alpha}\right)^{-\beta}. \qquad (6)$$

Eq. 6 essentially combines the log-normal approximation for the IMF derived by Chabrier (2003, 2005) with the Salpeter (1955) power-law slope for stars with mass $>1\,M_\odot$. Here, $\mu = 0.2\,M_\odot$ is the average stellar mass, $\alpha = 2.3$ is the Salpeter power-law exponent for higher mass stars, and $\beta = 1.4$ is the power-law exponent to describe the slope of the IMF for low-mass objects (which also deviates from the log-normal form; Bastian, Covey & Meyer 2010). Finally, we sample from this IMF within the mass range $m_{low} = 0.01\,M_\odot$ to $m_{up} = 50\,M_\odot$.

We note that in this paper, the choice of the mass distri-

bution is unimportant, because we are comparing the positions of the 10 most massive stars to the positions of all stars in a region. In this case, we only require the massive stars to have masses above those of the remaining 290 objects.

However, stochastic sampling of the IMF for low-N regions can result in very different mass distributions between realisations (Parker & Goodwin 2007), and if we were to study the subsequent dynamical evolution, differences in the relative masses of individual stars could affect the measured amount of mass segregation.

We created 20 realisations of the fractal distribution (and mass distribution). However, in the following we concentrate on just one typical realisation of the spatial distribution, and mass distribution of stars. The realisation is 'typical' in the sense that it nicely highlights the advantages, and disadvantages of each of the methods.

For each realisation we assign the stellar masses in one of three ways. First the stellar masses are randomly assigned, so no mass segregation – whatever the definition – should be detected (Section 3.1). We then change the positions of the ten most massive stars so that they are either more centrally concentrated (Section 3.2) or in the locations of the highest stellar surface density (Section 3.3).

We perform all the subsequent analysis in 2 dimensions in order to mimic the information available to observers.

It should be noted that *all* methods make a hidden assumption that the 2 dimensional distributions are a good representation of the true 3 dimensional structure (in the sense that they retain the same information on spatial distributions). It is unclear if this is really the case, and we will return to this difficult question in a later paper. For now we will proceed under the assumption that the 2 dimensional distributions do retain the important information present in the true 3 dimensional structure.

3.1 Random distributions of stellar masses

In this section we use our four techniques for measuring mass segregation on a random distribution of stars, as shown in Fig. 1. The locations of the ten most massive stars are shown by the large red dots.

3.1.1 Radial mass functions, $\mathcal{M}_{MF}$

In Fig. 2(a) we show the cumulative distribution of the radial distances from the centre of the fractal for all stars (the solid black line) and for the ten most massive stars (the red dashed line). Within 3 pc of the centre, the two distributions are overlaid. However, there are no massive stars at radii greater than 3.2 pc and the cumulative distributions differ beyond this radius. However, a KS test on the two distributions returns a p-value of 0.51 that the two populations share the same parent distribution, i.e. the difference is not significant in that it is higher than our threshold of $p = 0.1$.

It is important to note that the centre of the distribution is known to us to be at $\{0, 0\}$ pc. When confronted with a distribution similar to that shown in Fig. 1, an observer would use the average position of all the stars to define a centre. In the example shown here, this average position is almost identical to the centre of mass.
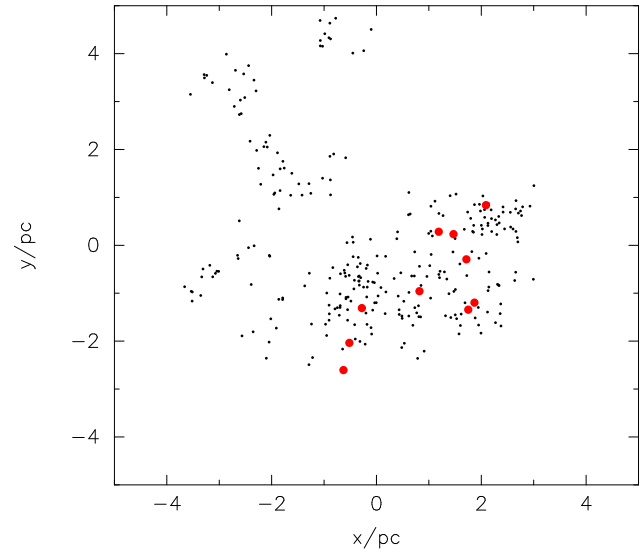
Figure 1. A fractal distribution ($D = 2.0$) with stars randomly drawn from an initial mass function and placed randomly in the spatial distribution. The ten most massive stars are shown by the larger (red) points.

3.1.2 Mass segregation ratio, Λ_{MSR}

In Fig. 2(b) we show Λ_{MSR} as a function of the N_{MST} stars for the fractal region in Fig 1. $\Lambda_{MSR} = 1$ (consistent with there being no mass segregation) is shown by the horizontal red dashed line. The Λ_{MSR} technique shows that the 10 most massive stars are slightly more centrally concentrated than the average stars, with $\Lambda_{MSR} = 1.7^{+0.3}_{-0.4}$ for stars with $m > 2.05$. The 20 most massive stars are also slightly more centrally concentrated than the average stars.

This positive signal of mass segregation is likely due to the same spatial feature in Fig. 1 that shows an apparent difference in the radial mass functions, namely that none of the most massive stars are more than 3 pc from the centre (Fig. 2(a)). This is a 2-σ difference from unity, and so would be expected roughly 1-in-20 times. By 'fluke' this is the only random realisation that shows a 2-σ signature of mass segregation and emphasises the need to avoid over-interpreting a single 2-σ result.

3.1.3 Local density ratio, Σ_{LDR}

In Fig. 2(c) we plot the local stellar surface density, Σ, against individual stellar mass m in Fig. 2(c). The median stellar surface density for the entire distribution is 13.1 stars pc^{-2} (the blue dashed line) whereas the median stellar surface density for the ten most massive stars is 13.2 stars pc^{-2} (the solid red line). These values are obviously very similar, and a KS test returns a p-value of 0.3 that they share the same parent distribution – i.e. this is not a significant difference compared to our threshold value of $p = 0.1$. $\Sigma_{LDR} = 1.0$ and we therefore conclude that the most massive stars are not mass segregated according to this definition.
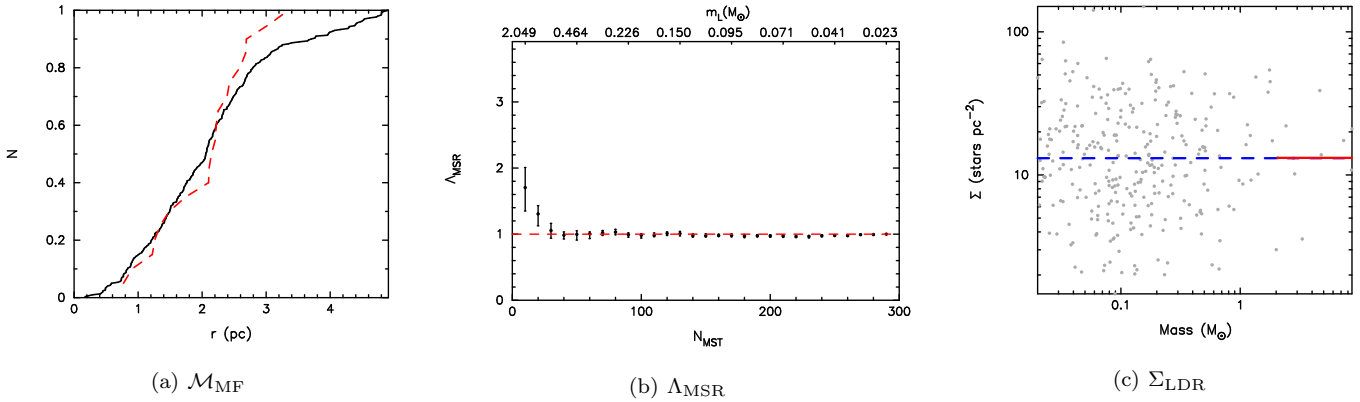
Figure 2. Three separate measures of mass segregation for the stellar distribution shown in Fig. 1. In panel (a) we show the cumulative distribution of the distance from the centre for the ten most massive stars (the red dashed line) and the cumulative distribution for all stars (the solid black line) – the mass function comparison, $\mathcal{M}_{\mathrm{MF}}$. In panel (b) we show the Λ_{MSR} mass segregation ratio as a function of the N_{MST} stars used in the subset (the lowest mass star, m_L, for various N_{MST} values is shown along the top horizontal axis). $\Lambda_{\mathrm{MSR}} = 1$ (i.e. no preferred spatial distribution) is shown by the solid horizontal red dashed line. In panel (c) we show local stellar surface density versus stellar mass (the $\Sigma - m$ plot). The median stellar surface density for the ten most massive stars is shown by the righthand solid (red) horizontal line and the median surface density for all of the stars is shown by the blue horizontal dashed line.

3.1.4 Group segregation ratio, Ω_{GSR}

In Fig. 3 we show the determination of the Ω_{GSR} group segregation ratio. We start by constructing an MST of the entire region, as shown in Fig. 3(a). The cumulative distribution of the branches in the entire MST is shown in Fig. 3(b), and the two power law fits to the close branches and the long branches are shown by the solid red lines. Following Gutermuth et al. (2009); Kirk & Myers (2011) and Kirk et al. (2014) we take the intersection of these lines as the MST $d_{\mathrm{break}} = 0.28$ pc, the boundary between 'clustered' and 'diffusely' distributed stars. All MST branches with length $< d_{\mathrm{break}}$ are retained (Fig. 3(c)) which defines groups within the distribution[3].

In Fig. 3(c) we show the groups (with $N > 2$) selected by this method as the stars still connected by the red MST links. The most massive star *within each of the groups* is marked by a red triangle. The ten most massive stars in the entire region are shown by the large open blue circles.

It might be considered that $d_{\mathrm{break}} = 0.28$ pc has a physical importance – it is the apparent break between structures. However, in this simulation this distance has no physical significance, it is just a projected 5 pc radius $D = 2.0$ box fractal distribution, which by design is hierarchical and self-similar, with no special spatial scale (apart from the radius itself). Examination of Fig. 3 shows that there is nothing 'special' about this distance. Furthermore, small changes to d_{break} can drastically affect the number of groups which are identified. For example, if we choose $d_{\mathrm{break}} = 0.25$ pc (the point at which the cumulative distribution in Fig. 3(b) deviates from the steep power-law), we identify 18 groups (instead of the 16 identified using $d_{\mathrm{break}} = 0.28$ pc). If we choose $d_{\mathrm{break}} = 0.5$ pc (where the shallow power-law slope deviates from the tail of the distribution), we identify only 6 groups.

Examination of Fig. 1 shows to the eye perhaps five groups, the most significant being to the bottom right. Fig. 3(c) shows that Ω_{GSR} has identified many more groups than this. In particular, the stars to the bottom left (around $\{-3, -1\}$ pc) have been split into three groups. And the significant distribution of stars at the bottom centre/right have been split into several groups, but some stars (including one of the most massive in the region) have not been included in any group.

The identification of groups is crucial to the Ω_{GSR} method, but it is unclear from Fig. 3(c) that the selected groups are 'real' in any sense.
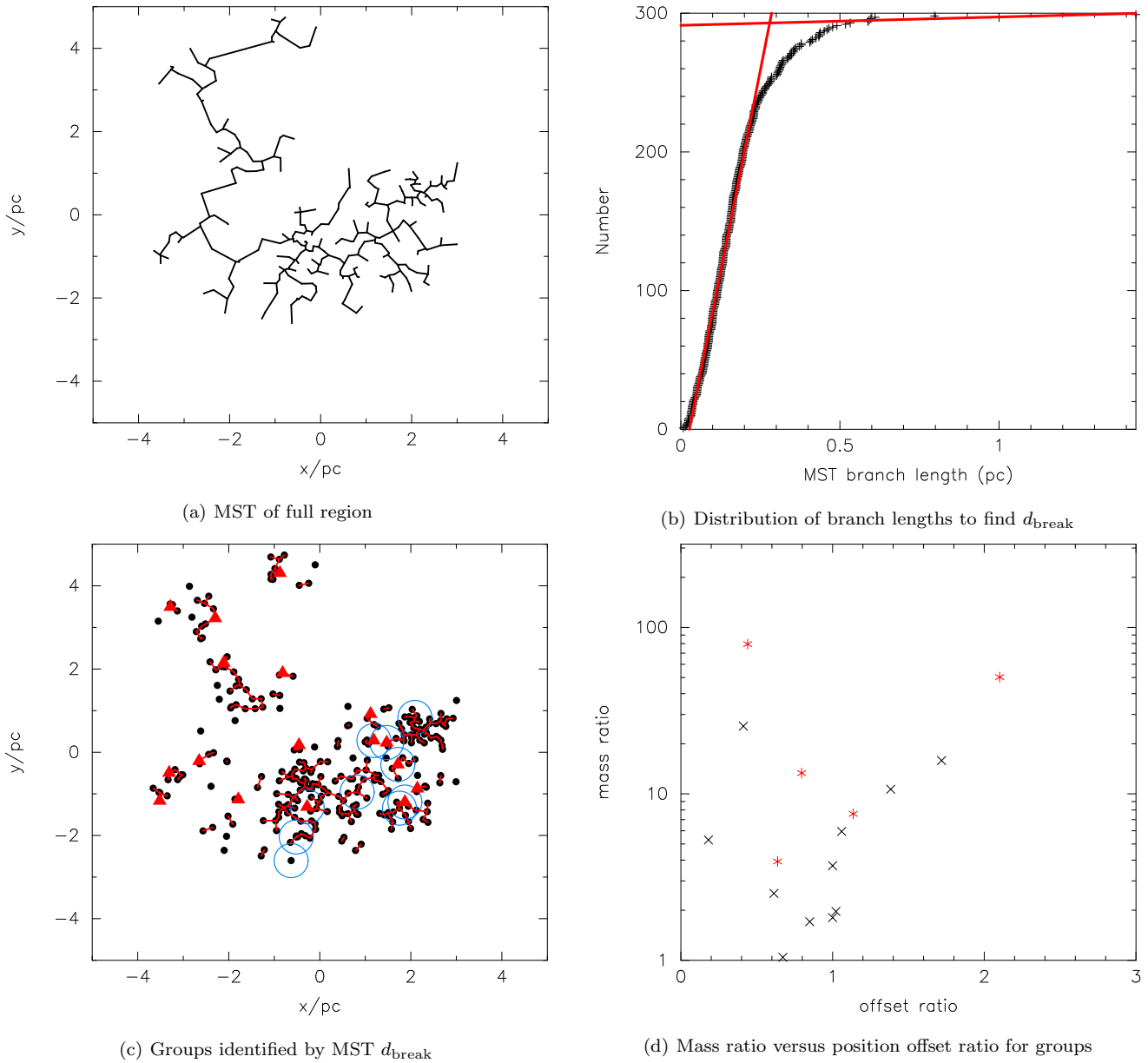
There are three other significant issues with the Ω_{GSR} method that are immediately apparent from Fig. 3(c).

Firstly, the most massive star in a group may not be one of the most massive stars in the region. All of the groups to the upper left have a locally most massive star that is not one of the most massive stars in the region as a whole.

Secondly, a group may contain more than one of the truly most massive stars in a region (e.g. three of the larger groups to the bottom right) in which case only the most massive of these is considered and the other (truly massive for the region) stars are discarded.

Thirdly, if a truly massive star is not part of a group (surely an interesting phenonena) then it is discarded from the analysis entirely (e.g. the large open blue circle at the bottom centre).

But taking the Ω_{GSR} method to its conclusion we show the mass ratio (most massive star in the group to median star in the group) versus offset ratio (position of most massive star to median group position) in for all groups with $N > 2$ stars in Fig. 3(d). The five groups with $N \geqslant 10$ stars are shown by the red points, and three of them have an offset ratio less than unity, i.e. they are mass segregated according to the definition in Kirk & Myers (2011) and Kirk et al. (2014). We define the group segregation ratio as the number of groups with an offset ratio less than or equal to unity divided by the total number of groups. For all groups

---

[3] Other methods to define groups/clusters in crowded fields may have advantages over the MST technique – see Schmeja (2011) for a review.

(a) MST of full region

(b) Distribution of branch lengths to find d_{break}

(c) Groups identified by MST d_{break}

(d) Mass ratio versus position offset ratio for groups

Figure 3. Mass segregation as defined by the Ω_{GSR} method. In panel (a) an MST of the full spatial distribution is shown, and the cumulative distribution of all of the branch lengths is shown in panel (b). The two power law slopes used to fit the data are shown by the red lines. The intersection of these slopes gives the critical MST length, d_{break}, and in panel (c) we show the groups identified using this length. In the groups in which there are 3 or more stars the most massive star in the group is shown by the solid red triangle. The positions of the ten most massive stars in the *full distribution* are shown by the large open blue circles (these correspond to the filled red circles in Fig. 1). In panel (d) we show the mass ratio of the most massive star in each group to the group median mass versus the ratio of the position of the most massive star to the median position of the group. Groups with ten or more stars are shown by the red asterisks.

with $N > 2$, $\Omega_{\mathrm{GSR}} = 0.59$ and for groups with $N \geqslant 10$, $\Omega_{\mathrm{GSR}} = 0.60$[4]. In a truly random distribution, $\Omega_{\mathrm{GSR}} = 0.5$.
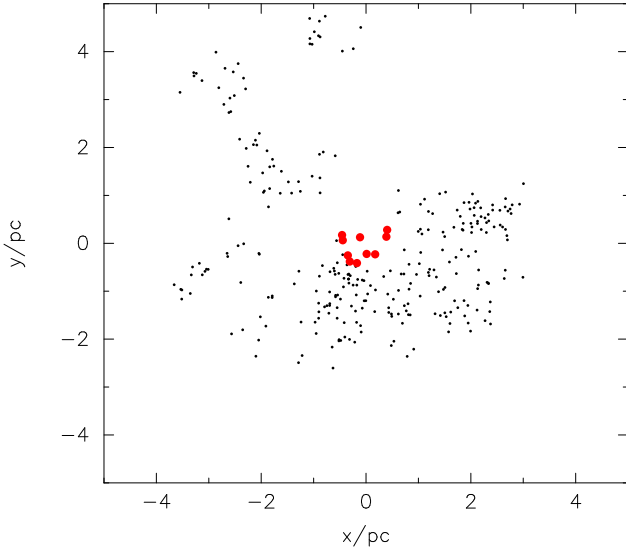
It is worth noting another problem here, in that the Ω_{GSR} method needs to define a 'centre' of each group from which to measure distances. Therefore there is an implicit

---

[4] Note that Kirk & Myers (2011) and Kirk et al. (2014) generally only present statistics for groups containing 10 or more stars, and we will also draw conclusions based only on these 'large' groups.

assumption of spherical symmetry which examination of Fig. 3(c) shows not to be the case in most groups.

There are two groups with $N \geqslant 40$ stars, which is enough points to run the Λ_{MSR} and Σ_{LDR} methods on these groups in isolation. One of these groups has an offset ratio of less than unity (i.e. it is mass segregated according to this method) – however, neither Λ_{MSR} nor Σ_{LDR} find mass segregation in this group. The second group has an offset ratio of greater than unity (i.e. it is *inversely* mass segregated ac-

Figure 4. As Fig. 1; a fractal distribution of stellar masses randomly drawn from an initial mass function. However, in this case we have swapped the locations of the ten most massive stars (shown by the larger red points) with the ten most central stars.

cording to this method). Again, both Λ_{MSR} and Σ_{LDR} are consistent with no mass segregation (normal or inverse).

3.2 Massive stars centrally concentrated

We now swap the positions of the 10 most massive stars with the positions of the 10 stars closest to the centre of the fractal distribution, as shown by the red points in Fig. 4. This is clearly a rather artificial distribution of the most massive stars, but it is one that most closely matches the 'classical' definition of mass segregation for this region.

3.2.1 Radial mass functions, $\mathcal{M}_{\mathrm{MF}}$

In Fig. 5(a) the cumulative distribution of radial positions of the 10 most massive stars is shown by the red dashed line, whereas the cumulative distribution of the radial positions for all stars is shown by the solid black line. Due to the central concentration of the most massive stars, the KS test returns a p-value of 2×10^{-4} that the two subsets share the same parent distribution.

This result demonstrates that if we have confidence in the definition of the centre of a region, a strong mass segregation signature may still be seen in substructured distributions using the radial mass function technique.

3.2.2 Mass segregation ratio, Λ_{MSR}

We show the Λ_{MSR} ratio in Fig. 5(b). The ten most massive stars have $\Lambda_{\mathrm{MSR}} = 5.3^{+0.9}_{-1.0}$, which is significantly above unity. In 20 realisations, only 1 star-forming region displays a Λ_{MSR} ratio that is not significantly above unity, with values ranging from $\Lambda_{\mathrm{MSR}} = 2.0^{+0.3}_{-0.4}$ to $\Lambda_{\mathrm{MSR}} = 11.1^{+1.1}_{-1.4}$.

This is completely unsurprising as Λ_{MSR} is designed to measure exactly this type of mass segregation – the most massive stars being much closer to one-another than a random sample of stars would be.

3.2.3 Local density ratio, Σ_{LDR}

Interestingly, the Σ_{LDR} ratio does not reflect the central concentration of the 10 most massive stars. $\Sigma_{\mathrm{LDR}} = 0.58$ due to the most centrally located stars being in areas of relatively low surface density, although a KS test returns a p-value of 0.26 that the massive stars have a different parent distribution to the full distribution (i.e. this difference is not significant). That said, most people would conclude simply from eye that the distribution shown in Fig. 4 is mass segregated, even though the massive stars have low local surface density. In 20 realisations of this distribution, Σ_{LDR} does not detect mass segregation in 11, and in a further 5 it finds inverse mass segregation.

3.2.4 Group segregation ratio, Ω_{GSR}

The overall spatial distribution has not changed between Figs. 1 and 4 and so the determination of d_{break} and the subsequent identification of groups is identical to that in Section 3.1. We show the groups defined by d_{break} in Fig. 6(a), noting the change of location of the 10 most massive stars in the full distribution (the blue open circles). The locations of the most massive star in each group (shown by the red triangles) have also changed in some cases.

Again, we note that two of the 10 most massive stars from the full distribution are now no longer part of a group with $N > 2$, and instead are in a pair (located at $\{0.4, 0.1\}$ pc). We show the mass ratio versus offset ratio for all groups with $N > 2$ stars in Fig. 6(b). Again, the five groups with $N \geqslant 10$ stars are shown by the red points. This time only two of these five groups are mass segregated ($\Omega_{\mathrm{GSR}} = 0.40$), even though the global distribution of massive stars is very mass segregated.

In this situation – where the most massive stars in a region are 'centrally' concentrated, it is not clear what Ω_{GSR} is measuring. The majority of the measurements of mass ratio versus offset ratio do not include any of the ten most massive stars in the region.

3.3 Massive stars in areas of high density

We now change the positions of the massive stars once more, and swap them with stars with the highest local surface densities, as shown by the red points in Fig. 7. In this case we are shifting from a type of mass segregation related to 'classical' mass segregation to one in which the massive stars are associated with the highest density regions (at least surface density; the volume densities of these locales would be unknown to the hypothetical observer).
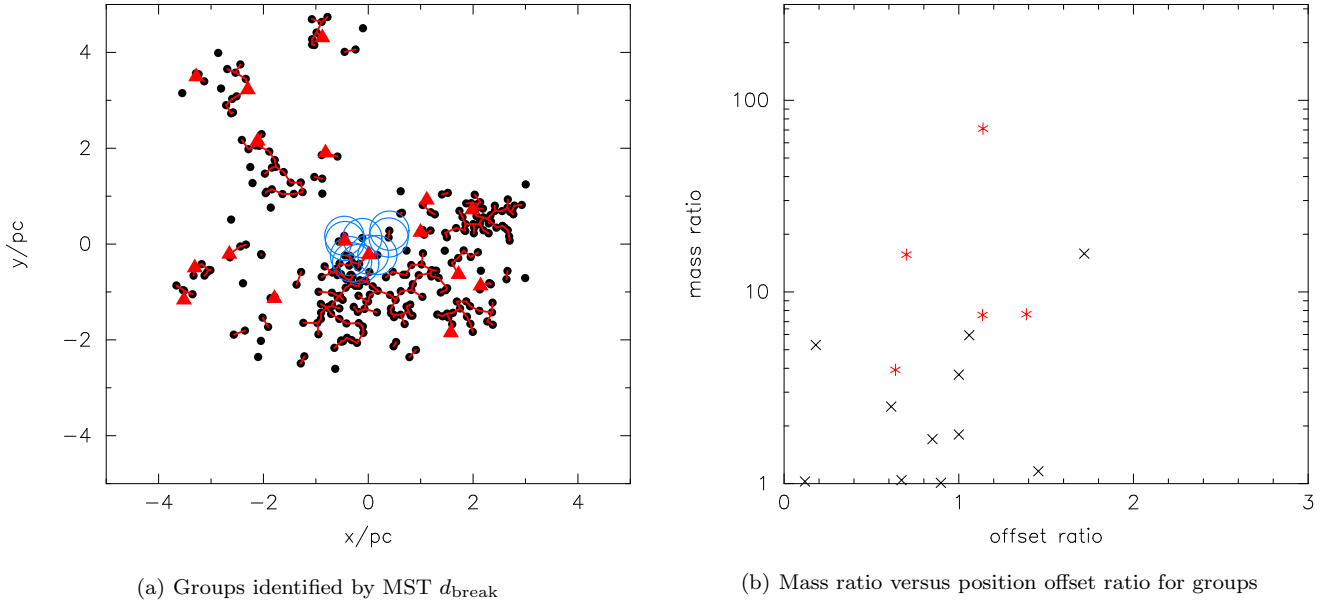
3.3.1 Radial mass functions, $\mathcal{M}_{\mathrm{MF}}$

The radial mass function for the 10 most massive stars (the red dashed line) and the whole distribution (the black solid line) is shown in Fig. 8(a). As for the centrally concentrated cluster, the most massive stars are closer to the centre (none are outside of 3.3 pc) than the average stars, and a KS test returns a p-value of 7×10^{-3} that they share the same underlying parent distribution. However, in 13 of our 20 realisations in which we draw different masses and positions for the stars each time, the KS test returns a p-value in excess

(a) $\mathcal{M}_{\mathrm{MF}}$

(b) Λ_{MSR}

(c) Σ_{LDR}
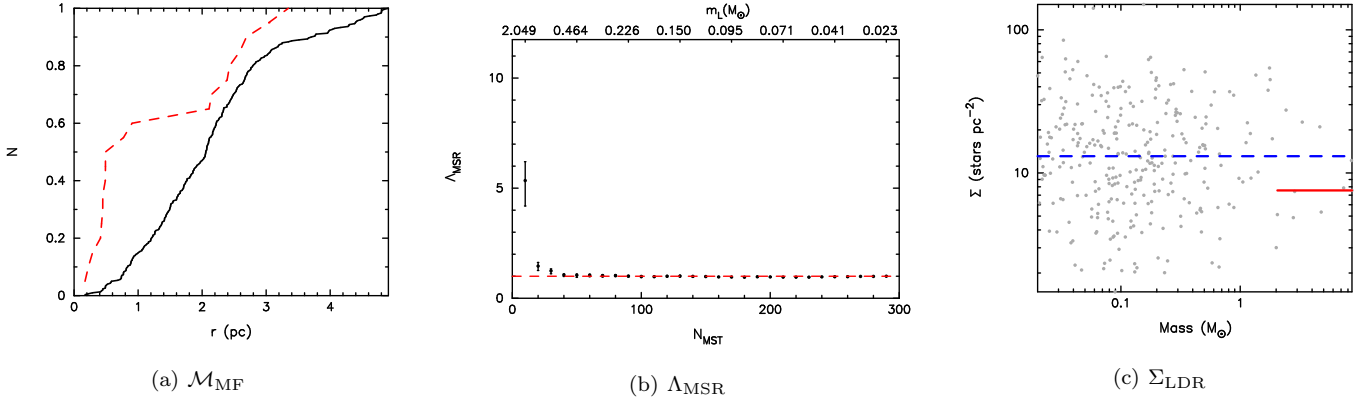
Figure 5. Three separate measures of mass segregation for the stellar distribution shown in Fig. 4 where the most massive stars are centrally concentrated. In panel (a) we show the cumulative distribution of the distance from the centre for the ten most massive stars (the red dashed line) and the cumulative distribution for all stars (the solid black line) – the mass function comparison, $\mathcal{M}_{\mathrm{MF}}$. In panel (b) we show the Λ_{MSR} mass segregation ratio as a function of the N_{MST} stars used in the subset (the lowest mass star, m_L, for various N_{MST} values is shown along the top horizontal axis). $\Lambda_{\mathrm{MSR}} = 1$ (i.e. no preferred spatial distribution) is shown by the solid horizontal red dashed line. In panel (c) we show local stellar surface density versus stellar mass (the $\Sigma - m$ plot). The median stellar surface density for the ten most massive stars is shown by the righthand solid (red) horizontal line and the median surface density for all of the stars is shown by the blue horizontal dashed line.


(a) Groups identified by MST d_{break}

(b) Mass ratio versus position offset ratio for groups

Figure 6. Mass segregation as defined by the Ω_{GSR} method for the stellar distribution shown in Fig. 4 where the most massive stars are centrally concentrated. The stellar groups are identified as shown in Fig. 3(a) and Fig. 3(b). In panel (a) we show the groups identified using MST d_{break}. In the groups in which there are 3 or more stars the most massive star in the group is shown by the solid red triangle. The positions of the ten most massive stars in the *full distribution* are shown by the large open blue circles (these correspond to the filled red circles in Fig. 4). In panel (d) we show the mass ratio of the most massive star in each group to the group median mass versus the ratio of the position of the most massive star to the median position of the group. Groups with ten or more stars are shown by the red asterisks.

of 0.1, suggesting that the massive stars are not closer to the centre than the average members. This is not entirely surprising, as the positions in the region with the highest surface density may not be co-located, as is the case for one of the massive stars in Fig. 7.

3.3.2   Mass segregation ratio, Λ_{MSR}

We show the measurement of Λ_{MSR} for this distribution in Fig. 8(b). The 10 most massive stars have $\Lambda_{\mathrm{MSR}} = 2.7^{+0.4}_{-0.6}$, i.e. mass segregation is present according to this measure, but is not as strong as in the case where we placed the most massive stars at the centre of the distribution.

In many ways this is not surprising. Stars with the highest surface density are reasonably likely to be close to one-
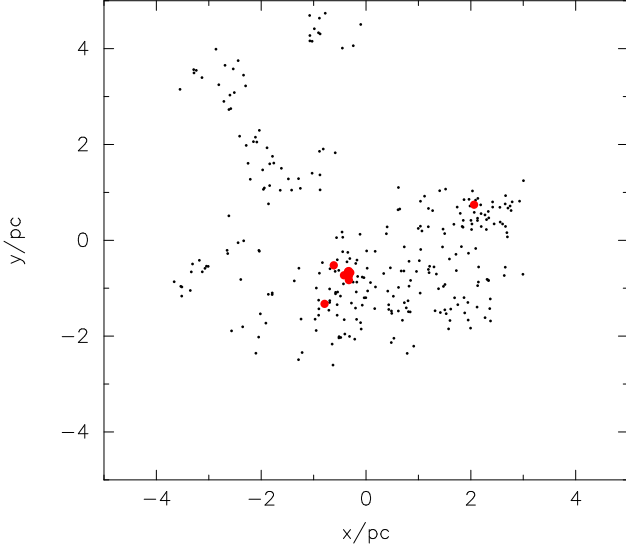
Figure 7. As Fig. 1; a fractal distribution of stellar masses randomly drawn from an initial mass function. However, in this case we have swapped the locations of the ten most massive stars (shown by the larger red points) with the ten stars with the highest local stellar surface densities (as defined by Eq. 3).

another (as the surface density is high), and so this artifical set-up will often place several massive stars close to one-another (here at $\{-0.5, -0.7\}$ pc). This is not always the case, from 20 realisations of this distribution, in 11 the measured Λ_{MSR} was greater than unity, but less than two (and only marginally significant, error bars typically being around ± 0.5).

3.3.3 Local density ratio, Σ_{LDR}

When we compare the surface density of the most massive stars to the average surface density, unsurprisingly the most massive stars have much higher median values, as shown in Fig. 8(c). Here, the most massive stars have $\Sigma = 64.1$ stars pc^{-2}, compared to $\Sigma = 13.1$ stars pc^{-2} for the region average. $\Sigma_{LDR} = 4.9$, and a KS test returns a p-value of 8×10^{-7} that they share the same underlying parent distribution.

This is exactly as expected as the set-up is such that Σ_{LDR} should find mass segregation by its definition of it.

3.3.4 Group segregation ratio, Ω_{GSR}

As in Section 3.2 and shown in Fig. 6, MST d_{break} is the same as that calculated in Section 3.1 because the spatial distribution has not changed. The groups identified by MST d_{break} are shown in Fig. 9(a), and the most massive star in each group is shown by the red triangle. The 10 most massive stars in the distribution are shown by the blue circles. This time, none of these 10 massive stars are not in groups, but we have a significant problem that one group contains 9 of them (and so 8 will be discarded from the analysis). When we determine whether that group is mass segregated according to the Kirk & Myers (2011) method, we are effectively ignoring the positions of 8 of these stars. This time, three of the five groups with $N \geqslant 10$ are mass segregated, and

the largest group (containing 9 of our most massive stars in the full distribution) is also mass segregated according to Λ_{MSR} and Σ_{LDR}. However, the other large group (containing the single massive star) is not mass segregated according to the Kirk & Myers (2011) method, but it is with Λ_{MSR} and Σ_{LDR}. For the groups with $N > 2$, $\Omega_{GSR} = 0.59$, and for $N \geqslant 10$ $\Omega_{GSR} = 0.60$, i.e. more groups than not are mass segregated according to this method.

4   DISCUSSION

When attempting to find 'mass segregation' in a region it is absolutely critical to clearly define what is meant by 'mass segregation'. Confusion between apparently contradictory results for 'mass segregation' between different methods occurs because the different methods are searching for different things. For example, Maschberger & Clarke (2011) find mass segregation according to Σ_{LDR} in the hydrodynamical simulations of star formation from Bonnell et al. (2008), but do not find mass segregation with Λ_{MSR}. We contend that this is not condradictory, rather just different definitions of 'mass segregation' (e.g. Parker et al. 2014).

A definition of mass segregation based on relaxation and equipartition in a dynamically old system is one in which *the most massive stars are closer together than expected by random chance*. It is this definition that is proped by radial mass function methods ($\mathcal{M}_{MF}$) and Λ_{MSR}. In searching for this type of mass segregation Λ_{MSR} is more useful as it does not require a centre to be defined and can deal with complex (substructured) distributions.

The Σ_{LDR} method defines mass segregation differently – in this case mass segregation is that *the most massive stars are preferentially in regions of higher surface density than random*. Whilst this method does not measure 'mass segregation' in the classical sense, it is extremely useful for probing the past dynamical history of a star-forming region, as the most massive stars sweep up retinues of low-mass stars during the two-body relaxation of initially dense ($>100 \, M_\odot \, pc^{-3}$) regions (Parker et al. 2014; Parker 2014; Wright et al. 2014).

One way of avoiding confusion between Λ_{MSR} and Σ_{LDR} is to make the definition of mass segregation more stringent, for example that the most massive stars should be globally more concentrated *and* be at the centre of individual groups. However, this requires the somewhat arbitrary definition of groups, which is arguably impossible if all the stars formed in the same star formation 'event' in the same molecular cloud, and so any boundary between groups is necessarily artificial. Furthermore, as we have seen in Section 3.2 a spatial distribution that few would argue is not mass segregated would fail this definition.
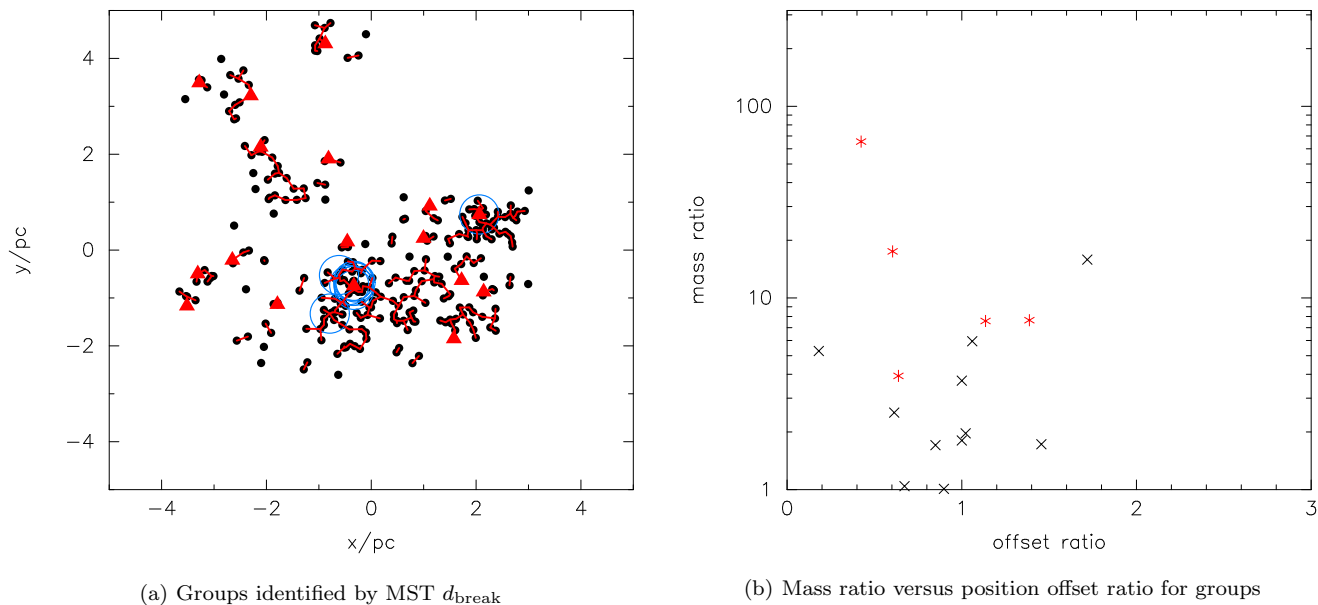
In this context it is unclear to the authors what exactly Ω_{GSR} is searching for, or what definition of 'mass segregation' it involves. We have also identified a number of problems with the Ω_{GSR} method which we feel makes it unsuitable for finding 'mass segregation'.

Firstly, it is unclear if the group identification is in any way finding 'real' groups.

Secondly, the identification of groups discards any stars that are not in an $N > 2$ group (or higher N, depending on the number of stars per group as defined in a particular

(a) $\mathcal{M}_{\mathrm{MF}}$

(b) Λ_{MSR}

(c) Σ_{LDR}
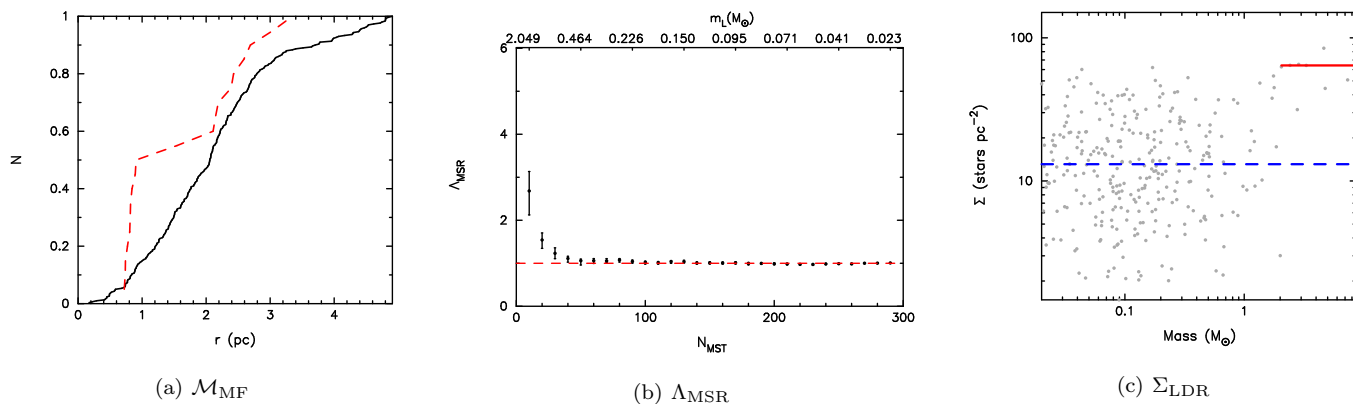
Figure 8. Three separate measures of mass segregation for the stellar distribution shown in Fig. 7 where the most massive stars are in the areas of highest stellar surface density. In panel (a) we show the cumulative distribution of the distance from the centre for the ten most massive stars (the red dashed line) and the cumulative distribution for all stars (the solid black line) – the mass function comparison, $\mathcal{M}_{\mathrm{MF}}$. In panel (b) we show the Λ_{MSR} mass segregation ratio as a function of the N_{MST} stars used in the subset (the lowest mass star, m_L, for various N_{MST} values is shown along the top horizontal axis). $\Lambda_{\mathrm{MSR}} = 1$ (i.e. no preferred spatial distribution) is shown by the solid horizontal red dashed line. In panel (c) we show local stellar surface density versus stellar mass (the $\Sigma - m$ plot). The median stellar surface density for the ten most massive stars is shown by the righthand solid (red) horizontal line and the median surface density for all of the stars is shown by the blue horizontal dashed line.

(a) Groups identified by MST d_{break}

(b) Mass ratio versus position offset ratio for groups

Figure 9. Mass segregation as defined by the Ω_{GSR} method for the stellar distribution shown in Fig. 7 where the most massive stars are in areas of highest stellar density. The stellar groups are identified as shown in Fig. 3(a) and Fig. 3(b). In panel (a) we show the groups identified using MST d_{break}. In the groups in which there are 3 or more stars the most massive star in the group is shown by the solid red triangle. The positions of the ten most massive stars in the *full distribution* are shown by the large open blue circles (these correspond to the filled red circles in Fig. 7). In panel (d) we show the mass ratio of the most massive star in each group to the group median mass versus the ratio of the position of the most massive star to the median position of the group. Groups with ten or more stars are shown by the red asterisks.

analysis, Kirk & Myers 2011; Kirk et al. 2014). This ignores many stars, removing them from further analysis, even if they are amoung the most massive stars in the region.

Thirdly, once groups have been identified the method only considers the most massive star in that group, discarding information on the masses of any other stars.

Forthly, groups are assumed to have a 'centre' from which distances can be measured, essentially performing a 'radial mass function' approach based on a single massive star in a small-N subset of the total population.

Finally, it is worth noting that small-N statistics can play an important role in obtaining any information from the Ω_{GSR} method. In the examples we showed above there are only five groups with $N > 10$. For no 'mass segregation' we would expect 2 or 3 to show no signal, however it would

not be unusual for only 0 or 1 to show no signal, or 4 or 5 to.

Variations on this final point is important for all methods. A positive signal for 'mass segregation' in-and-of-itself may not tell us much. As we saw in the example random distribution we used above (Section 3.1.2), Λ_{MSR} found mass segregation at 2-σ significance. This is a result we would expect 1-in-20 times, and examining our ensemble of simulations we find this is indeed the case (and some show 'inverse mass segregation' in which $\Lambda_{\mathrm{MSR}} < 1$). This 'random noise' effect has been seen in ensembles of simulations (see Parker et al. 2015).

Based on this, it is quite possible that small signatures of 'mass segregation' such as the apparently inverse mass segregation found by Parker et al. (2011) in Taurus might well have been over-interpreted and are quite possibly consistent with a random distribution of the most massive stars. This highlights the requirement for more than one technique to be applied to any search for mass segregation in an observed region.

5 CONCLUSIONS

We have experimented with four methods used to find 'mass segregation': the radial mass function method $\mathcal{M}_{\mathrm{MF}}$ (e.g. Sagar et al. 1988; Sabbi et al. 2008), Λ_{MSR} (Allison et al. 2009), Σ_{LDR} (Maschberger & Clarke 2011), and Ω_{GSR} (Kirk & Myers 2011). Our results can be summarised as follows.

(i) Only in smooth, spherical, centrally concentrated distributions (e.g. Plummer spheres) do all methods find 'mass segregation'. In more complex, substructured distributions different methods can find different things because they define 'mass segregation' differently.

(ii) Only Λ_{MSR} measures 'classical' mass segregation where the massive stars are concentrated in particular regions without having to define a cluster centre.

(iii) The radial mass function method $\mathcal{M}_{\mathrm{MF}}$ searches for 'classical' mass segregation, but requires a centre to be defined and then assumes spherical symmetry.

(iv) Σ_{LDR} measures a different 'mass segregation' where the massive stars are in regions of higher than average surface density without having to define a cluster centre. The massive stars may, or may not, also be concentrated together.

(v) Ω_{GSR} finds groups that may, or may not, be physically important and then defines a 'centre'. In doing so it can exclude very significant information on some of the most massive stars in a region (sometimes excluding them from the analysis entirely).

We conclude that of the methods currently in use, by far the most useful are Λ_{MSR} and Σ_{LDR}. They use all of the information on all of the stars in a region without assuming anything about the spatial distributions. We reiterate, however, that they measure different definitions of 'mass segregation' and so should be used in tandem.

Finally, we note that marginal signals of mass segregation (as found by any method) in observed star-forming regions may not have anything to do with the physics of star formation, and any analysis should be accompanied by a suite of simulations of synthetic regions like those presented here. In a future paper, we will also examine the potentially significant and serious problems of analysing projected distributions and attempting to extract information on the three dimensional properties.

REFERENCES

Allison R. J., Goodwin S. P., Parker R. J., Portegies Zwart S. F., de Grijs R., 2010, MNRAS, 407, 1098
Allison R. J., Goodwin S. P., Parker R. J., Portegies Zwart S. F., de Grijs R., Kouwenhoven M. B. N., 2009, MNRAS, 395, 1449
Ascenso J., Alves J., Lago M. T. V. T., 2009, A&A, 495, 147
Bastian N., Covey K. R., Meyer M. R., 2010, ARA&A, 48, 339
Beccari G., Lützgendorf N., Olczak C., Ferraro F. R., Lanzoni B., Carraro G., Stetson P. B., Sollima A., Boffin H. M. J., 2012, ApJ, 754, 108
Blaauw A., 1964, ARA&A, 2, 213
Bonnell I. A., Clark P. C., Bate M. R., 2008, MNRAS, 389, 1556
Bressert E., Bastian N., Gutermuth R., Megeath S. T., Allen L., Evans, II N. J., Rebull L. M., Hatchell J., Johnstone D., Bourke T. L., Cieza L. A., Harvey P. M., Merin B., Ray T. P., Tothill N. F. H., 2010, MNRAS, 409, L54
Carpenter J. M., Meyer M. R., Dougados C., Strom S. E., Hillenbrand L. A., 1997, AJ, 114, 198
Cartwright A., Whitworth A. P., 2004, MNRAS, 348, 589
Casertano S., Hut P., 1985, ApJ, 298, 80
Chabrier G., 2003, PASP, 115, 763
Chabrier G., 2005 Vol. 327 of Astrophysics and Space Science Library, The Initial Mass Function: from Salpeter 1955 to 2005. p. 41
Chavarría L., Mardones D., Garay G., Escala A., Bronfman L., Lizano S., 2010, ApJ, 710, 583
Dale J. E., Ercolano B., Bonnell I. A., 2012, MNRAS, 424, 377
Dale J. E., Ercolano B., Bonnell I. A., 2013, MNRAS, 430, 234
de Grijs R., Johnson R. A., Gilmore G. F., Frayn C. M., 2002, MNRAS, 331, 228
de Marchi G., Paresce F., 1996, ApJ, 467, 658
Delgado A. J., Djupvik A. A., Costado M. T., Alfaro E. J., 2013, MNRAS, 435, 429
Elmegreen B. G., Elmegreen D. M., 2001, AJ, 121, 1507
Er X.-Y., Jiang Z.-B., Fu Y.-N., 2013, Research in Astronomy and Astrophysics, 13, 277
Gieles M., Portegies Zwart S. F., 2011, MNRAS, 410, L6
Girichidis P., Federrath C., Allison R., Banerjee R., Klessen R. S., 2012, MNRAS, 420, 3264

Goodwin S. P., Whitworth A. P., 2004, A&A, 413, 929

Gouliermis D., Keller S. C., Kontizas M., Kontizas E., Bellas-Velidis I., 2004, A&A, 416, 137

Gouliermis D. A., de Grijs R., Xin Y., 2009, ApJ, 692, 1678

Gouliermis D. A., Hony S., Klessen R. S., 2014, MNRAS, 439, 3775

Gutermuth R. A., Megeath S. T., Myers P. C., Allen L. E., Fazio J. L. P. G. G., 2009, ApJS, 184, 18

Hillenbrand L. A., 1997, AJ, 113, 1733

Hillenbrand L. A., Hartmann L. W., 1998, ApJ, 492, 540

King I. R., 1966, AJ, 71, 64

Kirk H., Myers P. C., 2011, ApJ, 727, 64

Kirk H., Offner S. S. R., Redmond K. J., 2014, MNRAS, 439, 1765

Kruijssen J. M. D., 2012, MNRAS, 426, 3008

Küpper A. H. W., Maschberger T., Kroupa P., Baumgardt H., 2011, MNRAS, 417, 2300

Lada C. J., Lada E. A., 2003, ARA&A, 41, 57

Maschberger T., 2013, MNRAS, 429, 1725

Maschberger T., Clarke C. J., 2011, MNRAS, 416, 541

Moeckel N., Bonnell I. A., 2009, MNRAS, 396, 1864

Myers A. T., Klein R. I., Krumholz M. R., McKee C. F., 2014, MNRAS, 439, 3420

Olczak C., Spurzem R., Henning T., 2011, A&A, 532, 119

Pang X., Grebel E. K., Allison R. J., Goodwin S. P., Altmann M., Harbeck D., Moffat A. F. J., Drissen L., 2013, ApJ, 764, 73

Parker R. J., 2014, MNRAS, 445, 4037

Parker R. J., Bouvier J., Goodwin S. P., Moraux E., Allison R. J., Guieu S., Güdel M., 2011, MNRAS, 412, 2489

Parker R. J., Dale J. E., Ercolano B., 2015, MNRAS, 446, 4278

Parker R. J., Goodwin S. P., 2007, MNRAS, 380, 1271

Parker R. J., Wright N. J., Goodwin S. P., Meyer M. R., 2014, MNRAS, 438, 620

Pinfield D. J., Jameson R. F., Hodgkin S. T., 1998, MNRAS, 299, 955

Plummer H. C., 1911, MNRAS, 71, 460

Porras A., Christopher M., Allen L., Di Francesco J., Megeath S. T., Myers P. C., 2003, AJ, 126, 1916

Raboud D., Mermilliod J.-C., 1998, A&A, 333, 897

Rivilla V. M., Jiménez-Serra I., Martín-Pintado J., Sanz-Forcada J., 2014, MNRAS, 437, 1561

Sabbi E., Sirianni M., Nota A., Tosi M., Gallagher J., Smith L. J., Angeretti L., Meixner M., Oey M. S., Walterbos R., Pasquali A., 2008, AJ, 135, 173

Sagar R., Miakutin V. I., Piskunov A. E., Dluzhnevskaia O. B., 1988, MNRAS, 234, 831

Salpeter E. E., 1955, ApJ, 121, 161

Sana H., Momany Y., Gieles M., Carraro G., Beletsky Y., Ivanov V. D., De Silva G., James G., 2010, A&A, 515, A26

Sánchez N., Alfaro E. J., 2009, ApJ, 696, 2086

Schmeja S., 2011, AN, 332, 172

Schmeja S., Gouliermis D. A., Klessen R. S., 2009, ApJ, 694, 367

Schmeja S., Kumar M. S. N., Ferreira B., 2008, MNRAS, 389, 1209

Spitzer Jr. L., 1969, ApJL, 158, L139

Stolte A., Brandner W., Brandl B., Zinnecker H., 2006, AJ, 132, 253

Stolte A., Brandner W., Grebel E. K., Lenzen R., Lagrange A.-M., 2005, ApJL, 628, L113

Wright N. J., Parker R. J., Goodwin S. P., Drake J. J., 2014, MNRAS, 438, 639